The EuroBiotech Journal
RESEARCH ARTICLE
Medical Biotechnology

Two rare CHST3 missense variants, p.(Cys247Ser) and p.(Leu294Pro), in the homozygous and compound-heterozygous state cause chondrodysplasia with congenital joint dislocations in a consanguineous Syrian kindred

Julia Vodopiutz[1], Magdalena Felderer[2], Gabriel Floriani[3], Dietmar Rieder[3,4], Dorota Garczarczyk-Asim[2], Thomas Müller[2], Andreas R Janecke[2,5]*

Abstract

Biallelic loss-of-function variants in the carbohydrate sulfotransferase 3 gene (*CHST3*), which encodes chondroitin 6-O-sulfotransferase 1, cause an autosomal recessive skeletal dysplasia that unites the former entities recessive Larsen syndrome, humero-spinal dysostosis and spondyloepiphyseal dysplasia Omani type. The disorder presents with congenital dislocations of large joints and variable short stature and evolves into a progressive spondyloepiphyseal dysplasia; cardiac valve disease, hearing loss and dental anomalies occur in a subset of patients. We studied a six-generation consanguineous Syrian kindred with five affected individuals from three sibships clinically suspected with *CHST3*-related disease. Trio-exome sequencing in one nuclear family revealed homozygosity for the rare missense variant c.881T>C, p.(Leu294Pro) in exon 3 of *CHST3*. Direct Sanger sequencing of exon 3 in all three nuclear families confirmed homozygosity for p.(Leu294Pro) in affected individuals from the first nuclear family and compound-heterozygosity for p.(Leu294Pro) and another ultrarare variant, c.740G>C, p.(Cys247Ser), in affected persons from the other two nuclear families. Each variant was observed only once, in the heterozygous state, among more than 1.5 million alleles in the Genome Aggregation Database. The same two variants had been reported once in a child from another consanguineous family of Syrian origin, suggesting a regional founder effect. Cysteine 247 is invariant across vertebrate orthologues, and leucine 294 is replaced only by other hydrophobic residues. Both variants received high in silico pathogenicity scores, and elastic network modelling of a predicted protein structure indicated destabilization of the enzyme. Leucine 294 lies seven residues upstream of the 3'-phosphate binding motif for the sulfate donor, in the region where the functionally confirmed substitutions p.(Leu286Pro), p.(Arg304Gln) and p.(Leu307Pro) cluster. We classify both variants as likely pathogenic according to current variant interpretation guidelines. The family shows that recessive disease in consanguineous pedigrees can result from compound heterozygosity, so analysis pipelines should not rely solely on regions of homozygosity.

Keywords: *CHST3*; compound heterozygosity; Réunion paradox; variant interpretation; spondyloepiphyseal dysplasia

Introduction

Genetic skeletal disorders are a large and heterogeneous group of conditions that affect the development and growth of cartilage and bone. Their combined birth prevalence has been estimated at approximately 1 in 5,000, and their severity ranges from mild short stature or early-onset osteoarthritis to perinatally lethal forms [1, 2]. The 2019 revision of the Nosology and Classification of Genetic Skeletal Disorders listed 461 disorders in 42 groups, with the molecular basis known for 92% of them [3], and the 2023 revision expanded the classification to 771 entries associated with 552 genes [4]. A substantial part of this expansion is due to next-generation sequencing, which has accelerated the identification of disease genes but has also increased the number of rare variants that must be interpreted in individual families.

One group of the nosology comprises the sulfation disorders, in which defective sulfation of glycosaminoglycans (GAGs) in the cartilage extracellular matrix disturbs skeletal development [3-5]. Sulfation reactions are catalysed by sulfotransferases, which transfer a sulfate group from the universal donor 3'-phosphoadenosine 5'-phosphosulfate (PAPS) to hydroxyl or amino groups of their acceptors. Membrane-bound carbohydrate sulfotransferases (CHSTs) reside in the Golgi apparatus and modify glycoproteins, glycolipids and proteoglycans [6]. Chondroitin sulfate proteoglycans are the most abundant proteoglycans of cartilage, and the position of sulfation on their N-acetylgalactosamine (GalNAc)

[1] Department of Pediatrics and Adolescent Medicine, Medical University of Vienna, Vienna, Austria
[2] Department of Pediatrics I, Medical University of Innsbruck, Innsbruck, Austria
[3] Institute of Bioinformatics, Medical University of Innsbruck, 6020 Innsbruck, Austria
[4] Bioinformatics Core Facility, Medical University of Innsbruck, 6020 Innsbruck, Austria
[5] Institute of Human Genetics, Medical University of Innsbruck, Innsbruck, Austria

***Corresponding author:**
Andreas R. Janecke
E-mail: andreas.janecke@i-med.ac.at

DOI: 10.2478/ebtj-2026-0022

© 2026 Authors. This work was licensed under the Creative Commons Attribution-NonCommercial-NoDerivs 4.0 License.

residues determines their biological properties [5].

The *CHST3* gene (chromosome 10q22.1) encodes chondroitin 6-O-sulfotransferase 1 (C6ST-1; EC 2.8.2.17), which catalyzes the transfer of sulfate to position 6 of GalNAc in chondroitin and also shows some activity towards keratan sulfate [7]. C6ST-1 is a 479-amino-acid type II transmembrane protein with a short cytoplasmic N-terminus, a transmembrane helix (residues 21–38) and a luminal region that contains the sulfotransferase domain. Like other members of the sulfotransferase family, it carries two conserved PAPS-binding motifs, the 5'-phosphosulfate binding (5'-PSB) and the 3'-phosphate binding (3'-PB) motif [8]. Mice deficient in C6ST-1 have been generated and characterized [9].

Biallelic loss-of-function variants in *CHST3* were first identified in a large Omani kindred with spondyloepiphyseal dysplasia (SED) Omani type [10, 11]. Subsequent studies showed that patients previously diagnosed with recessive Larsen syndrome or humero-spinal dysostosis carry biallelic *CHST3* variants too, and that these labels describe age-dependent presentations of a single disorder [12-15]. The condition is now termed chondrodysplasia with congenital joint dislocations, *CHST3*-related (Online Mendelian Inheritance in Man, OMIM 143095), or *CHST3*-related skeletal dysplasia [16, 17]. Affected newborns typically present with dislocation or subluxation of the knees, hips and elbows, clubfeet and short stature. Joint dislocations tend to improve during childhood, whereas a progressive spondyloepiphyseal dysplasia with platyspondyly, kyphoscoliosis, degenerative arthropathy and truncal shortening develops later [15, 16]. Radiographic hallmarks include vertebral coronal clefts, a widening of the interpedicular distance from T12 to L1 and a bifid distal humerus [15-18]. Extraskeletal findings include cardiac valve dysplasia, which can be severe or even lethal, as well as hearing loss, microdontia and craniosynostosis [14, 15, 17-20].

More than 50 pathogenic *CHST3* variants have been reported to date, most of them missense variants located in exon 3, which encodes the sulfotransferase domain [17, 18]. Most published patients originate from populations with a high rate of consanguinity and are homozygous for their variant [18, 19, 21, 22]. In genetically isolated or highly consanguineous populations, a recessive disorder is usually expected to result from a single founder allele in the homozygous state. However, more than one pathogenic allele of the same gene can segregate in such populations. This is illustrated by the so-called "Réunion paradox" and by a Mexican village isolate with limb-girdle muscular dystrophy type 2A, in which one patient was compound heterozygous for the local *CAPN3* founder variant and a second pathogenic allele [23]. We report a consanguineous Syrian kindred in which the disorder is either caused by compound heterozygosity for two rare missense variants, which had previously been reported together in only one patient, also of Syrian origin [24], or by homozygosity for one of these variants, representing another example of the Réunion paradox.

Materials and Methods

Patients

The family originates from Syria and comprises six generations with several consanguineous unions (Figure 1). Five individuals in three sibships were affected: V-4 and V-5, V-7 and V-9 and VI-1. Individual V-9 was the index patient. The study was approved by the Ethics Committee of the Medical University of Innsbruck, approval no. UN4501 and conducted according to the Declaration of Helsinki. Written informed consent for genetic testing and for publication was obtained from all participants or their legal guardians. Written consent for showing a patient image and patient's radiographs was obtained.

Genomic DNA was extracted from peripheral blood samples by standard methods; it was extracted from dried blood spots of the four members of IV-1, IV-2, V-4, V-5. A 3-mm disc was punched from each card, incubated in 0.2 M NaOH for 5 min at 75 °C and neutralized with 40 mM Tris-HCl in a volume of 100 µl. After mixing and centrifugation, 1µl the supernatant was used as a template for the polymerase chain reaction (PCR).

Exome sequencing

Exome sequencing was performed in the index patient (V-9) and his parents (IV-3, IV-4). Enrichment kit usage, sequencing platform, alignment to GRCh38 and GRCh37 reference sequences, variant calling and filtering strategy were reported [25]. Variants are described according to the reference transcript NM_004273.5 (ENST00000373115.5).

Variant segregation analysis by direct Sanger sequencing

Exon 3 of *CHST3* was amplified with primers 5'-CGACCTGTACGTGCTGGAGC and 5'-CGGATGCTCTCGCAGTTGC and checked for specificity using the Ensembl genome browser (release 115) and the In-Silico PCR tool of the University of California Santa Cruz (UCSC) genome browser. Both primers carried M13 tails at their 5' ends to allow sequencing with universal M13 primers (5'-ctaaaacgacggccagt and 5'-caggaaacagctatgac. Each 25-µl reaction contained 12.5 µl 2× GoTaq G2 Green Master Mix (Promega), 0.25 µl of each primer (Microsynth, Switzerland), 11 µl water and 1 µl template DNA. Cycling conditions were 95 °C for 3 min; 35 cycles of 95 °C for 20 s, 63 °C for 20 s and 72 °C for 30 s; and a final extension at 72 °C for 7 min (Veriti 96-Well Thermal Cycler, Applied Biosystems). A no-template control was included in each run. PCR products (6 µl) were separated on 2% agarose gels in Tris-borate-EDTA (TBE) buffer containing PeqGreen DNA/RNA dye (Peqlab) at 90–110 V for 45 min and visualised with a Gel Doc XR+ imaging system (Bio-Rad). PCR products were purified with ExoSAP-IT (Applied Biosystems; 37 °C for 30 min, 80 °C for 15 min) and sequenced bidirectionally with M13 forward and reverse primers using the BigDye Terminator v1.1 Cycle Sequencing Kit (Applied Biosystems). Sequencing reactions were purified on Sephadex G-50 Superfine (Cytiva) and run on an ABI 3730 DNA Analyzer. Chromatograms were aligned to the reference sequence using Sequencher 5.4.6 and CodonCode Aligner.

Variant assessment

Allele frequencies were retrieved from the Genome Aggregation Database (gnomAD, v4.1) [26]. Evolutionary conservation of the affected residues was assessed by aligning the human C6ST-1 sequence with orthologous sequences from seven vertebrate species (blue whale, saltwater crocodile, zebrafish, Ord's kangaroo rat, chicken, mouse and western clawed frog), selected from 199 orthologues listed in Ensembl. The functional impact of the missense variants was predicted with the ensemble method REVEL (Rare Exome Variant Ensemble Learner) [27] and with CADD (Combined Annotation Dependent Depletion) [28], as displayed in the gnomAD browser. Score thresholds for the computational evidence criterion PP3 followed the calibration of the Clinical Genome Resource (ClinGen) [29]. The three-dimensional structure of wild-type and mutant C6ST-1 was predicted with AlphaFold [30]. The effect of each substitution on protein dynamics and stability was estimated as the difference in vibrational entropy between wild-type and mutant ($\Delta\Delta S_{vib}$) using the Elastic Network Contact Model (ENCoM) [31]. Positive $\Delta\Delta S_{vib}$ values indicate increased flexibility and are interpreted as destabilizing [31, 32]. Variants were classified according to the guidelines of the American College of Medical Genetics and Genomics and the Association for Molecular Pathology (ACMG/AMP) [33], using the Bayesian point system proposed by Tavtigian et al. [34].

Results

Pedigree

The pedigree shows multiple consanguineous unions and five affected individuals in generations V and VI, all of whom were born to clinically unaffected parents, which is consistent with autosomal recessive inheritance (Figure 1).

Clinical features

The main presenting feature in all patients was congenital joint dislocations. When documented, all patients had congenital knee luxations bilaterally. The second most commonly affected joint was the elbow causing restriction of movement. Congenital hip dislocations and clubfeet were variably present. Most patients underwent multiple corrective surgeries in childhood. Patients developed lumbar or cervical kyphosis in late childhood. Birth length, when recorded, was above the third centile. The index patient was estimated to have normal stature when last seen at age 12 years, measures are incomplete due to multiple contractures of large and small joints (Figure 2).

Adult heights were below the third centile, e.g., the height of patient VI-1 was 126 cm (-6.54z) at age 17 years, with corresponding weight of 34.5 kg (-4.59z) and a head circumference of 54.1 cm (-0.94z). The height of patient V-7 was 126.3 cm (-6.04z) at age 18 years, with corresponding weight of 33.2 kg (-4.19z) and a head circumference of 55 cm (-0.54z). Where ex-

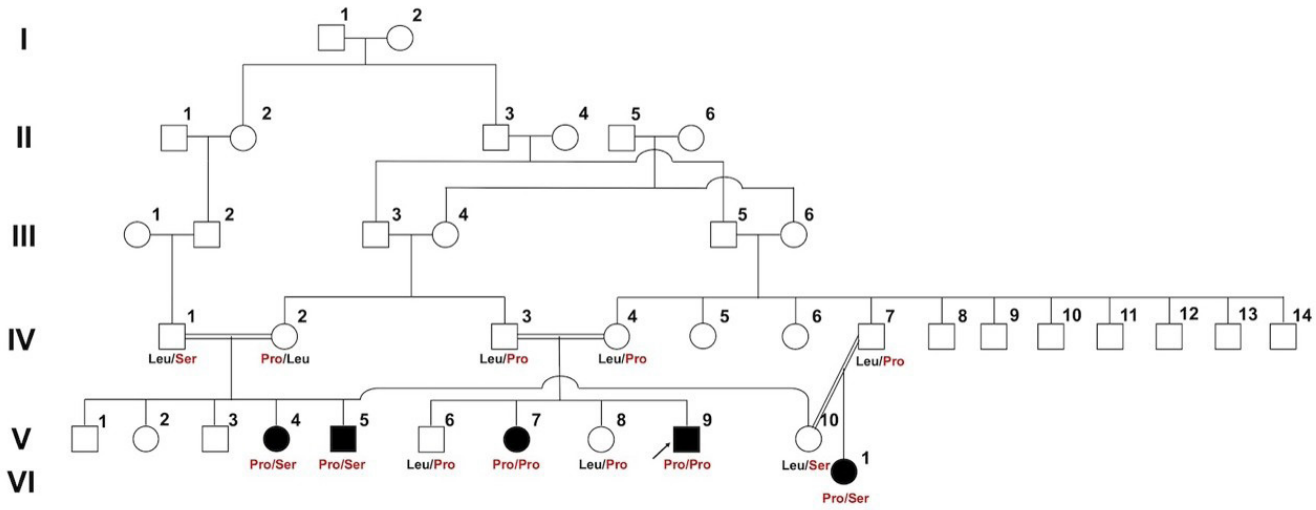


Figure 1. Pedigree of the studied kindred. Filled symbols denote affected individuals; double lines indicate consanguineous unions; the arrow marks the index patient (V-9). Exome sequencing was performed in sibship with patients V-7 & V-9. *CHST3* genotypes are shown below family members whose DNA samples were available with respect to amino acids encoded at codons 294 and 247, wild-type in black and mutations in red.



Figure 2. Clinical findings in the index patient (V-9 in Figure 1). Note the contractures of ankles, knees, hips, elbows. Radiographs show severe epiphyseal changes and the dislocation of long bones. A bifid distal humerus was documented bilaterally in all patients.

amined, patients presented with thickening of the mitral valve leaflets causing mild stenosis and mild insufficiency, as well as mildly thickened aortic valve. All patients had normal cognitive development and delayed acquisition of motor milestones because of joints dislocations and contractures.

The radiographic pattern is that of a progressive spondyloepiphyseal dysplasia but joint abnormalities are the predominant finding in childhood radiographs. The knee epiphyses are slightly smaller than average but generally well formed. The long bones themselves are well formed although there can be secondary changes related to joint misalignment. On lateral spine X-rays, there is superior and inferior notching on the vertebral bodies, reminiscent of partial coronal clefts but the vertebral bodies are normal in height. This finding is difficult to appreciate in later life and is also obscured if kyphosis develops. In contrast with dominant Larsen syndrome, patients with *CHST3* deficiency do not have broad thumbs and bone age is either delayed or normal.

The clinical features in the presented patients suggested *CHST3*-related disease and molecular testing was ordered for diagnosis confirmation.

Molecular testing results

Filtering for rare biallelic variants in genes associated with skeletal dysplasias identified the homozygous *CHST3* missense variant c.881T>C (p.(Leu294Pro)) in the index patient V-9, and each of his parents was heterozygous for this variant. Subsequently, Sanger sequencing of *CHST3* exon 3 was performed in all three sibships of this kindred. This type of segregation analysis showed homozygosity for p.(Leu294Pro) in the proband's affected sibling V-7 as well, and heterozygosity for this variant in his healthy siblings, supporting pathogenicity of this variant.

Affected individuals in the two other consanguineous unions from this kindred were compound-heterozygous for the p.(Leu294Pro) missense variant and a c.740G>C (p.(Cys247Ser)) variant in the same exon of *CHST3* (Figure 1, Figure 3). Each healthy parent was a carrier of either p.(Leu294Pro) or p.(Cys247Ser). Variants are described according to the reference transcript NM_004273.5 (ENST00000373115.5). Collectively, these two CHST3 missense mutations segregated with disease in the family.

Population frequency, conservation and in silico prediction

Both variants were extremely rare in gnomAD v4.1.2 (Table 1). The c.740G>C variant was observed once, in the heterozygous state, in a non-Finnish European individual (allele count 1/1,601,358; allele frequency 6.2×10^{-7}), and c.881T>C was observed once, in the heterozygous state, in another non-Finnish European individual (1/1,565,896; 6.4×10^{-7}). No homozygotes were recorded for either variant. Both variants have been reported once before, in the compound-heterozygous state, in a 4-year-old girl (patient F3P1) from a consanguineous Syrian family [24]. Homozygosity for either variant has not been re-

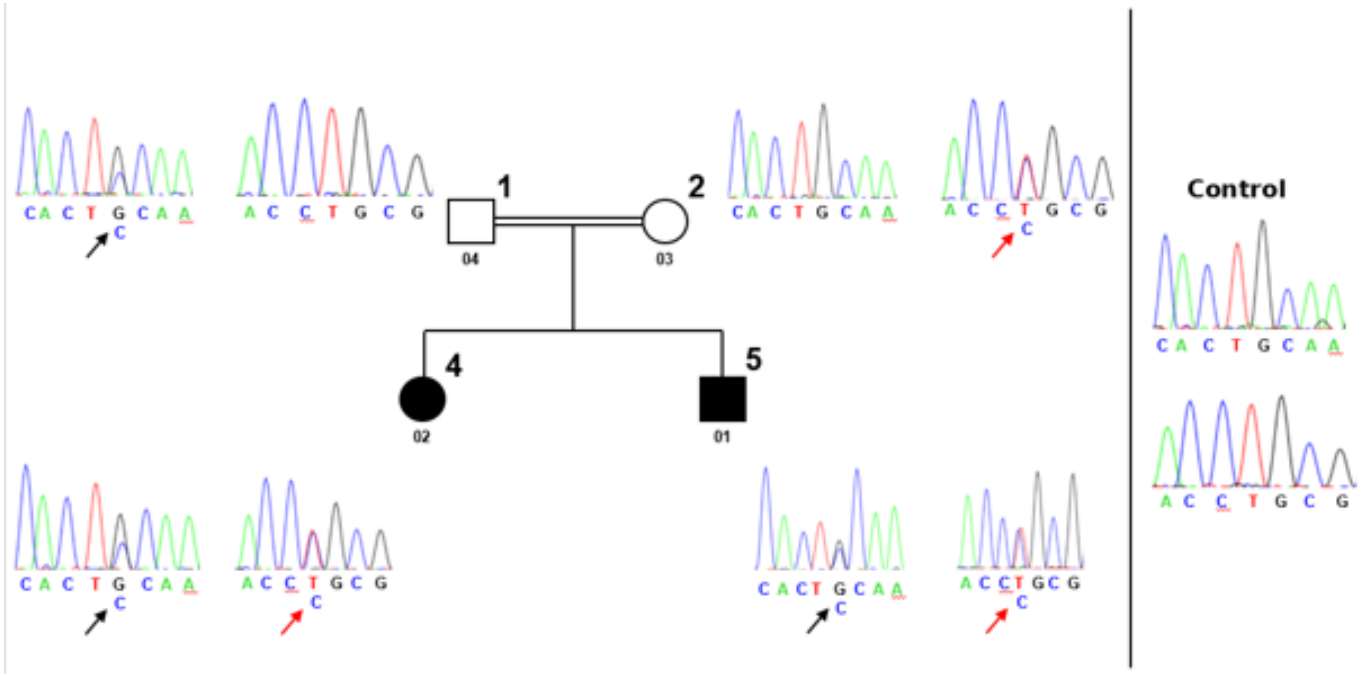


Figure 3. Representative Sanger sequencing chromatogram snippets showing segregation of *CHST3* exon 3 missense variants in one nuclear family from the kindred. For each individual, the left chromatogram shows the region around c.740 (black arrow) and the right chromatogram the region around c.881 (red arrow); the variant base is indicated below the reference base. The father (1, IV-1) is heterozygous for c.740G>C, the mother (2, IV-2) is heterozygous for c.881T>C, and both affected children (4, V-4; 5, V-5) are compound heterozygous. Reference chromatograms of a healthy control are shown on the right. NM_004273.5.

Table 1. Characteristics of the two *CHST3* variants identified in the family (NM_004273.5).

Feature	Variant 1	Variant 2
cDNA change	c.740G>C	c.881T>C
Protein change	p.(Cys247Ser)	p.(Leu294Pro)
Codon change	TGC > TCC	CTG > CCG
Exon / domain	Exon 3 / sulfotransferase domain	Exon 3 / sulfotransferase domain, 7 residues upstream of the 3'-PB motif
gnomAD v4.1 allele count / allele number	1 / 1,601,358	1 / 1,565,896
gnomAD allele frequency	6.2×10^{-7}	6.4×10^{-7}
gnomAD homozygotes	0	0
Conservation (7 vertebrate orthologues)	Invariant cysteine	Leu (4/7), Met (2/7), Val (1/7); hydrophobic in all
REVEL	0.851	0.909
CADD (PHRED)	26.4	31.0
ENCoM $\Delta\Delta S_{vib}$ (kcal·mol^{-1}·K^{-1})	+0.620 (destabilising)	+0.254 (destabilising)
ACMG/AMP classification	Likely pathogenic	Likely pathogenic

3'-PB, 3'-phosphate binding motif of PAPS; $\Delta\Delta S_{vib}$, difference in vibrational entropy between wild type and mutant.

Table 2. Multiple sequence alignment of human C6ST-1 with vertebrate orthologues around the two affected residues (bold; residues 241–264 and 288–307).

Species	Residues 241–264 (Cys247)	Residues 288–307 (Leu294)
Homo sapiens	VFEKYH**C**KNRRCGPLNVTLAAEAC	EDPRLD**L**RVIQLVRDPRAVL
Balaenoptera musculus	VFEKYP**C**KNRRCGLLNMTLAAEAC	EDPRLD**L**RVIQLVRDPRAVL
Crocodylus porosus	VFEKYH**C**KNRQCGPLNVTLAAEAC	EDPRLD**M**RIIQLVRDPRAVL
Danio rerio	IFERYH**C**KTRRCGPLNLTMASEAC	EDPRLD**V**KLIQLVRDPRAIL
Dipodomys ordii	VFEKYH**C**KNRRCGPLNVTLAAEAC	EDPRLD**L**RIIQLVRDPRAVL
Gallus gallus	VFEKYH**C**KNRRCGPLNITLAAEAC	EDPRLD**L**RVIQLVRDPRAVL
Mus musculus	VFEKYH**C**RNRRCGPLNVTLAGEAC	EDPRLD**L**RVIQLVRDPRAVL
Xenopus tropicalis	VFERYH**C**KNRRCGPLNMTLAMEAC	EDPRLD**M**RIIQLVRDPRAVL

Orthologous sequences were obtained from Ensembl (release 115).

Table 3. Classification of the *CHST3* variants according to the ACMG/AMP guidelines using the point-based system [33, 34].

Criterion	Evidence	c.740G>C	c.881T>C
PM2_Supporting	Allele count 1 in gnomAD v4.1, no homozygotes	+1	+1
PM3_Supporting	In trans with the second rare *CHST3* variant (phase confirmed by parental testing) in affected individuals	+1	+1
PP1	Co-segregation with disease in 3 (5) affected individuals from 2 (3) sibships	+1	+1
PP3_Moderate	REVEL 0.851 / 0.909 (≥ 0.773) [28]	+2	+2
PP4	Phenotype highly specific for *CHST3*-related skeletal dysplasia	+1	+1
Total points		6	6
Classification	6–9 points: likely pathogenic	LP	LP

LP, likely pathogenic. Functional evidence (PS3) is not yet available. PM3 was applied at supporting strength because the variant in trans was itself not yet classified as (likely) pathogenic.

ported in the *CHST3* literature to date [15, 17, 18, 24].

Cysteine 247 was invariant in all seven vertebrate orthologues examined, from mammals to zebrafish (Table 2). At position 294, leucine was present in four species, whereas methionine (crocodile, frog) or valine (zebrafish) were found in the others. Position 294 therefore tolerates only substitutions by other hydrophobic, helix-compatible residues, and the flanking residues, including Leu292 and the Asp-Pro-Arg motif at positions 302–304, were conserved in all species (Table 2). Both variants received high scores in the in silico tools: REVEL 0.851 and CADD 26.4 for p.(Cys247Ser), and REVEL 0.909 and CADD 31.0 for p.(Leu294Pro). According to the ClinGen calibration, both REVEL scores fall within the interval that provides moderate evidence of pathogenicity (0.773–0.932) [29].

Location of the variants and structural modelling

Both variants affect the sulfotransferase domain, in which most of the 50 pathogenic *CHST3* variants reported so far are located (Figure 4; Supplementary Table S1). Leu294 lies seven residues upstream of the 3'-PB motif (residues 301–309), in a segment that also contains the previously reported substitutions p.(Leu286Pro), p.(Asp302His), p.(Arg304Gln) and p.(Leu307Pro) [12,14,16,21]. Cys247 is located in a region between the two PAPS-binding motifs in which the pathogenic variants p.(Leu259Pro) and p.(Cys264Tyr) and p.(Cys264Ser) have been reported [12, 15, 17].

In the AlphaFold model, Cys247 lies in a loop close to Cys229, and its side chain engages in interactions that are lost when serine is introduced (Figure 5A). ENCoM predicted a positive $\Delta\Delta S_{vib}$ of 0.620 kcal·mol^{-1}·K^{-1} for p.(Cys247Ser), indicating increased molecular flexibility and destabilisation. Leu294 is located within an α-helix, and ENCoM predicted a $\Delta\Delta S_{vib}$ of 0.254 kcal·mol^{-1}·K^{-1} for p.(Leu294Pro), again indicating increased flexibility (Figure 5B). Proline cannot act as a hydrogen-bond donor to the backbone and its cyclic side chain restricts the backbone dihedral angles. It is therefore a strong helix breaker when introduced into the middle of an α-helix and is expected to disturb the local secondary structure.

Applying the ACMG/AMP criteria with the point-based framework, both variants met PM2_Supporting (absent or extremely rare in population databases), PM3_Supporting (detected in trans with a second rare variant in the same gene in affected individuals), PP1 (co-segregation with disease in several affected individuals in two and three sibships, respectively, of the same kindred), PP3_Moderate (REVEL ≥ 0.773) and PP4 (phenotype highly specific for a disease with a single genetic aetiology) (Table 3). This results in six points each, which corresponds to the classification "likely pathogenic".

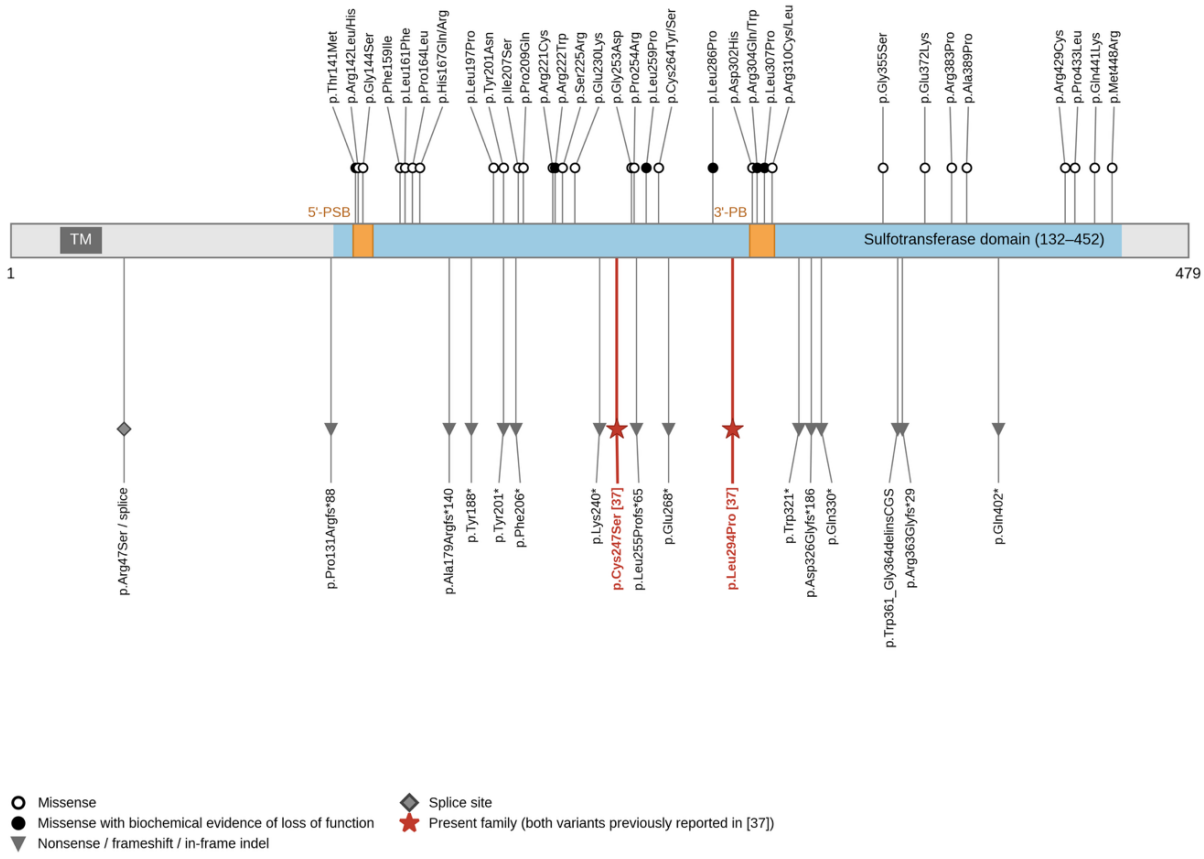


Figure 4. Spectrum of pathogenic *CHST3* variants. Schematic representation of chondroitin 6-O-sulfotransferase 1 (479 amino acids; UniProt Q7LGC8) with the transmembrane helix (TM), the sulfotransferase domain (residues 132–452) and the 5'-phosphosulfate binding (5'-PSB) and 3'-phosphate binding (3'-PB) motifs for PAPS. All 50 disease-associated variants that we identified in the literature are shown: missense variants above the protein (filled circles, variants with biochemical evidence of loss of function) and nonsense, frameshift, in-frame indel and splice-site variants below. Different substitutions of the same residue are combined in one label. The two variants of the present family are shown in red. Sources for each variant are listed in Supplementary Table S1 [11–23,34–38].

Discussion

We describe a consanguineous Syrian family in which *CHST3*-related chondrodysplasia with congenital joint dislocations is caused by homozygosity for a p.(Leu294Pro) variant in two patients, and by compound-heterozygosity for p.(Leu294Pro) and p.(Cys247Ser) missense variants in three patients. Both variants had previously been observed only once, in the compound-heterozygous state, in a single Syrian patient (F3P1) reported by Duz and Topak, who classified them as likely pathogenic on the basis of in silico predictions and parental carrier testing [24]. Our kindred provides the first segregation data for these variants across several affected individuals and, to our knowledge, the first observation of homozygosity for p.(Leu294Pro). Several independent lines of evidence support their pathogenicity. First, the variants co-segregate with the disease. Second, both variants are extremely rare in the general population, each being seen only once among more than 780,000 individuals in gnomAD, and never in the homozygous state, consistent with an ultrarare autosomal recessive disorder. Third, both affect the sulfotransferase domain, in which the large majority of pathogenic *CHST3* variants are located [15, 17, 18]. Fourth, both are predicted to be deleterious by in silico tools with calibrated thresholds, and both are predicted to destabilize the protein.

The p.(Leu294Pro) substitution is of particular interest because it adds to a series of leucine-to-proline substitutions in C6ST-1 that have been reported in patients: p.(Leu197Pro) [21], p.(Leu259Pro) [12, 15, 24], p.(Leu286Pro) [13] and p.(Leu307Pro) [12, 15]. For three of them, loss of function has been demonstrated experimentally. Recombinant C6ST-1 carrying p.(Leu286Pro) retained less than 1% of wild-type activity, and 6-O-sulfated chondroitin was undetectable in the patients' fibroblasts [13]. For p.(Leu259Pro) and p.(Leu307Pro), C6ST activity in patient fibroblasts was almost absent [15]. Leu294 lies between Leu286 and the 3'-PB motif (residues 301–309), in which p.(Asp302His), p.(Arg304Gln) and p.(Leu307Pro) are located [12,16,21]. In the original Omani family, p.(Arg304Gln) markedly reduced the 6-O-sulfation of chondroitin sulfate [11], and it was suggested that p.(Leu286Pro) impairs activity because of its proximity to the binding site of the 3'-phosphate of

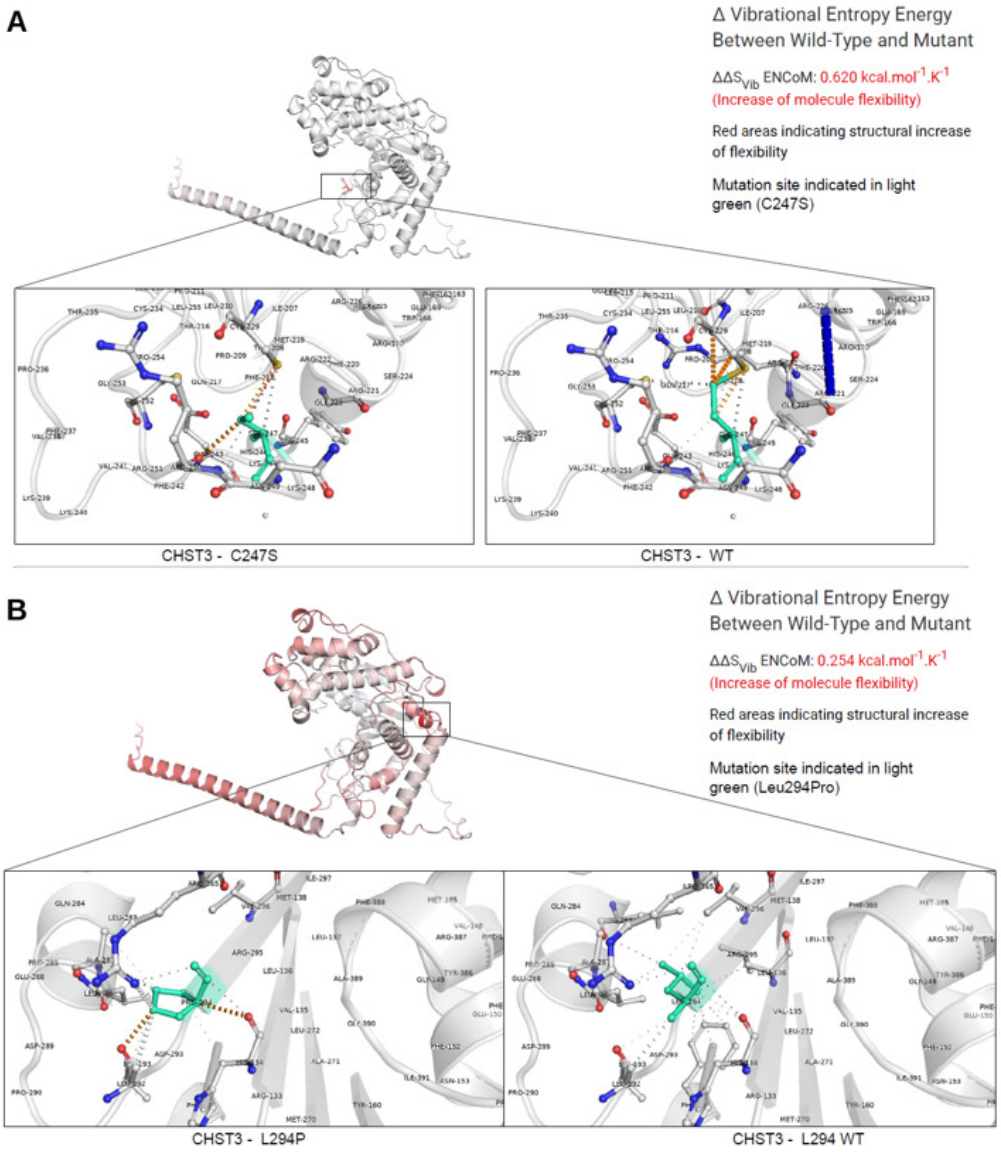


Figure 5. Predicted structural effects of the *CHST3* variants. The AlphaFold model rather than an experimentally determined model of C6ST-1 is shown with the mutated residue (light green) and the differences in vibrational entropy between wild type and mutant calculated with ENCoM (red, increased flexibility). (A) p.(Cys247Ser), $\Delta\Delta S_{vib}$ = +0.620 kcal·mol^{-1}·K^{-1}. (B) p.(Leu294Pro), $\Delta\Delta S_{vib}$ = +0.254 kcal·mol^{-1}·K^{-1}. Insets show the local environment of the mutant (left) and wild-type (right) residue.

PAPS [13]. Because Leu294 lies in an α-helix within this region, a proline at this position is expected to disrupt the helix and alter the geometry of the PAPS-binding pocket. The fact that position 294 is occupied only by hydrophobic residues (leucine, methionine, valine) in all vertebrates examined suggests that a hydrophobic, helix-compatible side chain is required there. Proline meets neither of these requirements.

Cys247 is invariant across the vertebrate orthologues we examined. Conserved cysteines in Golgi sulfotransferases often form intramolecular disulfide bonds that stabilize the luminal domain [8]. In our model, Cys247 lies close to Cys229, which is compatible with such a bond. However, this has not been confirmed experimentally, and the model does not allow us to decide whether the disulfide is formed. Replacement of cysteine by the smaller and more polar serine abolishes any disulfide bond and was predicted to increase flexibility and destabilise the protein. Pathogenic substitutions of cysteine 264, p.(Cys264Tyr) and p.(Cys264Ser), have been reported [15, 17], which further indicates that cysteine residues in this region are functionally important. Destabilizing missense variants frequently cause disease by loss of function [32], and loss of C6ST-1 activity is the established disease mechanism [11, 15]. However, the vibrational entropy changes calculated by ENCoM reflect predicted changes in protein dynamics and do not directly measure enzyme activity. Biochemical studies, for example measurement of C6ST activity and of the disaccharide composition of chondroitin sulfate in patient fibroblasts or of recombinant mutant enzymes, as performed for other variants [11, 13-15], would provide functional evidence (ACMG criterion PS3) and could raise the classification of both variants to

pathogenic.

Most published patients with *CHST3*-related skeletal dysplasia come from populations with high rates of consanguinity, such as those of Oman, Turkey, Egypt, Pakistan and India, and are homozygous for their causative variant (Table 4). In an Egyptian cohort, all 14 patients from 11 families were homozygous [17]. Compound heterozygosity is reported less often; it was found in several patients of rare multiethnic series and in a Chinese patient from a non-consanguineous family [12, 15, 35]. In our family, compound heterozygosity occurred in three patients despite parental consanguinity. Consanguinity increases the probability that a child is homozygous for an allele identical by descent [36], but in large, highly inbred kindreds more than one pathogenic allele of the same gene may segregate independently. A comparable situation was described in a Mexican population isolate with limb-girdle muscular dystrophy type 2A. There, 19 of 20 genotyped patients were homozygous for a novel *CAPN3* founder variant, whereas one patient was compound heterozygous for this variant and a second, previously known pathogenic allele. The authors attributed this allelic heterogeneity in a closed population to the introduction of additional founder alleles through sporadic immigration [23]. This phenomenon is known as the "Réunion paradox", where at least six different *CAPN3* mutations among patients with limb-girdle muscular dystrophy type 2A were identified in the original publication describing mutations in *CAPN3*, which encodes calpain-3, a calcium-activated neutral protease [37]. In such cases, analysis strategies that give priority to homozygous variants or to runs of homozygosity, as has been used successfully in *CHST3* families [20, 38], could miss the diagnosis. Our findings therefore support filtering for both homozygous and compound heterozygous variants in consanguineous families. In practice, the two variants in this kindred may have been introduced through different branches of the pedigree. Notably, the only other family known to carry these variants is also consanguineous and of Syrian origin, and the affected child F3P1 carries exactly the same allele combination, with p.(Cys247Ser) inherited from the father and p.(Leu294Pro) from the mother, as seen here [24]. The recurrence of two individually ultrarare alleles in two Syrian families points to a regional founder effect or to common ancestry of both families; whether the families are related is not known. Haplotype analysis of the *CHST3* region in both families could distinguish between these possibilities.

The clinical features of the affected individuals in our family correspond to the typical presentation of C6ST deficiency. They also closely resemble those of patient F3P1, the only other individual known to carry p.(Cys247Ser) and p.(Leu294Pro) [24]. At 4 years of age, she had short-trunk short stature, rhizomelia, bilateral fixed knee dislocations, elbow dislocations with cubitus valgus and bifid distal humeri, short metacarpals and brachydactyly, as well as irregular vertebral end plates and narrowed intervertebral spaces. As in our patients, the knees and elbows were the predominantly affected joints, whereas hip involvement and clubfeet were absent in F3P1 and only variably present in our family. Kyphosis and scoliosis were not yet present at age 4 years, consistent with the onset of kyphosis in late childhood in our patients. Hearing loss and cardiac involvement were not reported for F3P1 [24], whereas thickened mitral and aortic valves were found in our patients where examined. Congenital dislocations of the knees, hips and elbows, clubfeet and short stature are the leading features at birth, and the spinal changes become more prominent with age [15, 16]. The bifid distal humerus has been proposed as a key diagnostic sign [17, 18]. Adult height is usually between 110 and 135 cm [16], but it was considerably lower in a Pakistani kindred homozygous for a nonsense variant [19]. The patients from the kindred reported here were 8, 12, 18, 19, and 21 years old at last examination. We did not observe a correlation of the homozygous or compound-heterozygous CHST3 genotype with the extent of clinical findings, which might have been related to different residual activities of the mutant enzymes. Unger et al. found no correlation between mutation type and phenotype, and patients homozygous for truncating variants were not more severely affected than those with missense variants [15]. Marked intrafamilial variability has been described [17, 39]. Cardiac involvement, mainly thickening and insufficiency of the mitral, tricuspid and aortic valves, has been reported in many cohorts [14, 15, 18], and one Egyptian child died at four years of age from pulmonary hypertension and heart failure [17]. Hearing loss [13, 19], microdontia and delayed tooth eruption [10, 19] and sclerosis of the cranial sutures or craniosynostosis [19, 20] have also been reported. We therefore recommend echocardiography, audiological assessment and dental examination for all affected members of this family, in line with published recommendations [16, 18, 19].

The differential diagnosis of *CHST3*-related dysplasia includes other disorders with multiple congenital dislocations, in particular autosomal dominant Larsen syndrome caused by *FLNB* variants, Desbuquois dysplasia and the other sulfation disorders [3, 15, 41]. Normal or delayed bone age, the absence of a flat face and the characteristic vertebral changes help to distinguish CHST3 deficiency from these conditions [15]. Because the phenotype changes with age and overlaps with other conditions, molecular testing is essential for diagnosis and genetic counselling [17, 18]. Almost all reported pathogenic variants lie in exon 3 [17, 18]. Once the diagnosis is suspected clinically, or once the familial variants are known as in this kindred, targeted PCR and Sanger sequencing of the coding exons offers a rapid and inexpensive way to confirm the diagnosis and to test relatives. We showed that this approach works with DNA extracted from dried blood spots, which are easy to collect and ship. This is a practical advantage for families living far from specialised centres or in regions with limited laboratory resources. Advantages and disadvantages of this kind of sampling, and a comparison of commercial and non-commercial protocols for DNA extraction were recently evaluated [42]. Knowledge of both familial variants now allows carrier testing and genetic counselling of relatives in this extended consanguineous family, as well as prenatal or preimplantation genetic

Table 4. Published families with *CHST3*-related skeletal dysplasia whose variants are shown in Figure 3, compared with the present kindred (in chronological order).

Study	Origin	Patients / families	Genotype (NM_004273.5)	Notable findings
[10, 11]	Oman	Large kindred (2 related families)	Homozygous p.(Arg304Gln)	Progressive SED, severe kyphoscoliosis, arthropathy, microdontia; reduced 6-O-sulfation
[12]	Various	6 / 6	Homozygous or compound heterozygous: splice/p.(Arg47Ser), p.(Tyr201*), p.(Phe206*), p.(Arg222Trp), p.(Leu259Pro), p.(Leu307Pro), p.(Arg363Glyfs*29), p.(Glu372Lys)	Recessive Larsen syndrome, humero-spinal dysostosis; reduced C6ST activity in fibroblasts
[13]	Turkey	2 / 1	Homozygous p.(Leu286Pro)	Congenital dislocations, clubfeet, VSD, hearing loss; activity abolished in vitro
[14]	Turkey	3	Homozygous p.(Thr141Met)	SED Omani type, cardiac valve insufficiency; residual activity 24–29%
[15]	Multiethnic	24 / 23 (incl. 6 of Hermanns et al.)	24 variants, 16 patients homozygous; additionally p.(Arg142Leu), p.(Phe159Ile), p.(Leu161Phe), p.(His167Gln), p.(Ala179Argfs*140), p.(Ile207Ser), p.(Arg221Cys), p.(Ser225Arg), p.(Lys240*), p.(Gly253Asp), p.(Cys264Tyr), p.(Arg310Cys), p.(Gln330*), p.(Trp361_Gly364delinsCysGlySer), p.(Arg383Pro), p.(Arg429Cys)	Congenital dislocations and vertebral changes as key features; minor valve dysplasia in 5; no genotype–phenotype correlation
[39]	Somalia	2 half-siblings / 1	p.(Gly355Ser)	Marked intrafamilial variability
[19]	Pakistan	14 / 1	Homozygous p.(Glu268*)	Hearing loss in 6; very short adult height
[20]	India	3 / 3	Homozygous p.(Asp302His), p.(Pro164Leu), p.(Ala179Argfs*140)	Sclerosis of cranial sutures; severe valve disease
[38]	Afghanistan	1 fetus / 1	Homozygous p.(Pro164Leu)	Prenatal diagnosis: short long bones, dislocated knees, clubfeet
[40]	China	1 / 1	Homozygous p.(Pro209Gln)	SED with congenital joint dislocations; consanguineous parents
[24]	Turkey (4 families); Syria (1 family)	8 / 5	Homozygous p.(Leu259Pro) (2 families), p.(Tyr188*), p.(Trp321*); compound heterozygous p.(Cys247Ser) / p.(Leu294Pro) (consanguineous Syrian family)	Bifid distal humerus in 2; no hearing loss or cardiac involvement; literature review
[21]	Pakistan	15 / 3	Homozygous p.(Leu197Pro), p.(Tyr201*), p.(Arg221Cys)	SED with joint dislocations
[17]	Egypt	14 / 11	Homozygous p.(Pro131Argfs*88), p.(Arg142His), p.(Arg221Cys), p.(Arg222Trp), p.(Leu255Profs*65), p.(Cys264Ser), p.(Arg304Trp), p.(Arg310Leu), p.(Gln402*), p.(Gln441Lys)	Bifid distal humerus in all; microdontia; ASD; lethal cardiac disease
[35]	China	1 / 1	Compound heterozygous p.(Pro254Arg) / p.(Met448Arg)	Progressive joint pain; systematic review
[18]	India	9 / 5	Homozygous p.(Gly144Ser), p.(His167Arg), p.(Glu230Lys), p.(Asp326Glyfs*186), p.(Ala389Pro)	Bifid humerus, supernumerary carpal centres, valve anomalies
[22]	Pakistan	1 / 1	Homozygous p.(Tyr201Asn)	SED with congenital joint dislocations; facial dysmorphism
[16]	Amish (USA)	Founder population	p.(Pro433Leu)	Founder variant
Present study	Syria	5 affected / 3 sibships	Homozygous p.(Leu294Pro) (one sibship); compound heterozygous p.(Cys247Ser) / p.(Leu294Pro) (2 sibships)	Bilateral congenital knee dislocations, elbow involvement, kyphosis from late childhood, adult height 126 cm (VI-1), thickened mitral and aortic valves

ASD, atrial septal defect; C6ST, chondroitin 6-O-sulfotransferase; SED, spondyloepiphyseal dysplasia; VSD, ventricular septal defect. Numbers of patients refer to affected individuals reported in each publication.

testing if requested.

There is currently no causal therapy for *CHST3*-related skeletal dysplasia. Management is symptomatic and multidisciplinary, including orthopedic treatment of dislocations, clubfeet and spinal deformities, pain management and surveillance of cardiac and hearing function [16, 35]. Treatment with recombinant growth hormone is not recommended because of insufficient efficacy and a possible worsening of scoliosis [35].

This study has limitations. No functional studies of the mutant enzymes were performed, so the evidence for pathogenicity relies on genetic, population and computational data. The structural analysis is based on a predicted model and not on an experimentally determined structure. Finally, not all available family members have been genotyped so far, and further segregation analysis would strengthen the co-segregation evidence [43].

Conclusions

We report two rare missense variants in *CHST3*, c.740G>C, p.(Cys247Ser), and c.881T>C, p.(Leu294Pro), in the compound-heterozygous state in several but not all affected individuals from a consanguineous Syrian kindred with chondrodysplasia with congenital joint dislocations. Both variants segregate with the disease, are extremely rare in the general population, affect conserved positions of the sulfotransferase domain and are predicted to destabilise the enzyme; we classify them as likely pathogenic. Both variants had previously been reported only once, in a child from another consanguineous Syrian family, which suggests a founder effect. Our findings provide the first segregation evidence for both variants and add homozygosity for p.(Leu294Pro) to the known disease-causing genotypes of *CHST3*. They show that compound heterozygosity must be considered in consanguineous families, and that targeted Sanger sequencing of DNA from dried [42] blood spots is a robust and low-cost tool for the diagnosis and family testing of this rare skeletal dysplasia.

Acknowledgements

none

Conflict of interest statement

The authors declare that they have no conflict of interest.

Ethical review and approval

The study was reviewed and approved by the Ethics Committee of the Medical University of Innsbruck, approval no. UN4501. All participants or their legal guardians gave written informed consent for genetic testing and for the publication of the data.

Author contributions

J.V., A.R.J.: Conceptualization, Investigation, Formal analysis, Writing – original draft, review & editing, Visualization, Validation; D.G.-A., M.F., G.F., D.R.: Methodology, Investigation, Formal analysis, Software, T.M.: Resources, Project administration; all authors have contributed to manuscript production, and reviewed the material, and agreed to its content.

Supplementary Table S1. *CHST3* variants reported in patients with *CHST3*-related skeletal dysplasia (NM_004273.5), ordered by protein position. Variants detected in the present family are shown in bold.

cDNA	Protein	Type	Reference(s)
c.141G>C (with IVS2-1G>C)	p.(Arg47Ser)	Splice site / missense	[12, 15]
c.384_391dup	p.(Pro131Argfs*88)	Truncating / indel	[17]
c.422C>T	p.(Thr141Met)	Missense	[14]
c.425G>T	p.(Arg142Leu)	Missense	[15]
c.425G>A	p.(Arg142His)	Missense	[17]
c.430G>A	p.(Gly144Ser)	Missense	[18]
c.475T>A	p.(Phe159Ile)	Missense	[15]
c.481C>T	p.(Leu161Phe)	Missense	[15]
c.491C>T	p.(Pro164Leu)	Missense	[20, 38]
c.501C>A	p.(His167Gln)	Missense	[15]
c.500A>G	p.(His167Arg)	Missense	[18]
c.533_534insG	p.(Ala179Argfs*140)	Truncating / indel	[15, 20]
c.564C>A	p.(Tyr188*)	Truncating / indel	[24]
c.590T>C	p.(Leu197Pro)	Missense	[21]
c.601T>A	p.(Tyr201Asn)	Missense	[22]
c.603C>A	p.(Tyr201*)	Truncating / indel	[12, 15, 21]
c.617_618delinsGA	p.(Phe206*)	Truncating / indel	[12, 15]
c.620T>G	p.(Ile207Ser)	Missense	[15]
c.626C>A	p.(Pro209Gln)	Missense	[40]
c.661C>T	p.(Arg221Cys)	Missense	[15, 17, 21]
c.664C>T	p.(Arg222Trp)	Missense	[12, 15, 17]
c.675C>A	p.(Ser225Arg)	Missense	[15]
c.688G>A	p.(Glu230Lys)	Missense	[18]
c.718A>T	p.(Lys240*)	Truncating / indel	[15]
c.740G>C	**p.(Cys247Ser)**	Missense (this study)	[24], This study
c.758G>A	p.(Gly253Asp)	Missense	[15]
c.761C>G	p.(Pro254Arg)	Missense	[35]
c.763dup	p.(Leu255Profs*65)	Truncating / indel	[17]
c.776T>C	p.(Leu259Pro)	Missense	[12, 15, 24]
c.791G>A	p.(Cys264Tyr)	Missense	[15]
c.790T>A	p.(Cys264Ser)	Missense	[17]
c.802G>T	p.(Glu268*)	Truncating / indel	[19]
c.857T>C	p.(Leu286Pro)	Missense	[13]
c.881T>C	**p.(Leu294Pro)**	Missense (this study)	[24], This study
c.904G>C	p.(Asp302His)	Missense	[20]
c.911G>A	p.(Arg304Gln)	Missense	[10, 11]
c.910C>T	p.(Arg304Trp)	Missense	[17]
c.920T>C	p.(Leu307Pro)	Missense	[12, 15]
c.928C>T	p.(Arg310Cys)	Missense	[15]
c.929G>T	p.(Arg310Leu)	Missense	[17]
c.963G>A	p.(Trp321*)	Truncating / indel	[24]
c.976dup	p.(Asp326Glyfs*186)	Truncating / indel	[18]
c.988C>T	p.(Gln330*)	Truncating / indel	[15]
c.1063G>A	p.(Gly355Ser)	Missense	[39]
c.1083_1090delinsCGGCA	p.(Trp361_Gly364delinsCysGlySer)	Truncating / indel	[15]
c.1086del	p.(Arg363Glyfs*29)	Truncating / indel	[12, 15]
c.1114G>A	p.(Glu372Lys)	Missense	[12, 15]
c.1148G>C	p.(Arg383Pro)	Missense	[15]
c.1165G>C	p.(Ala389Pro)	Missense	[18]
c.1204C>T	p.(Gln402*)	Truncating / indel	[17]
c.1285C>T	p.(Arg429Cys)	Missense	[15]
c.1298C>T	p.(Pro433Leu)	Missense	[16]
c.1321C>A	p.(Gln441Lys)	Missense	[17]
c.1343T>G	p.(Met448Arg)	Missense	[35]

Functional (biochemical) evidence of loss of function has been reported for p.(Thr141Met), p.(Arg222Trp), p.(Leu259Pro), p.(Leu286Pro), p.(Arg304Gln) and p.(Leu307Pro). The list is based on the cited publications; variants reported only in supplementary material of reviews or in databases may be missing.

References

1. Geister, K.A. and S.A. Camper, *Advances in Skeletal Dysplasia Genetics.* Annu Rev Genomics Hum Genet, 2015. 16: 199–227.
2. Krakow, D. and D.L. Rimoin, *The skeletal dysplasias.* Genet Med, 2010. 12(6): 327–41.
3. Mortier, G.R., et al., *Nosology and classification of genetic skeletal disorders: 2019 revision.* Am J Med Genet A, 2019. 179(12): 2393–2419.
4. Unger, S., et al., *Nosology of genetic skeletal disorders: 2023 revision.* Am J Med Genet A, 2023. 191(5): 1164–1209.
5. Mizumoto, S. and S. Yamada, *Congenital Disorders of Deficiency in Glycosaminoglycan Biosynthesis.* Front Genet, 2021. 12: 717535.
6. Begolli, G., et al., *Carbohydrate sulfotransferases: a review of emerging diagnostic and prognostic applications.* Biochem Med (Zagreb), 2023. 33(3): 030503.
7. Fukuta, M., et al., *Molecular cloning and expression of human chondroitin 6-sulfotransferase.* Biochim Biophys Acta, 1998. 1399(1): 57–61.
8. Negishi, M., et al., *Structure and function of sulfotransferases.* Arch Biochem Biophys, 2001. 390(2): 149–57.
9. Uchimura, K., et al., *Functional analysis of the chondroitin 6-sulfotransferase gene in relation to lymphocyte subpopulations, brain development, and oversulfated chondroitin sulfates.* J Biol Chem, 2002. 277(2): 1443–50.
10. Rajab, A., J. Kunze, and S. Mundlos, *Spondyloepiphyseal dysplasia Omani type: a new recessive type of SED with progressive spinal involvement.* Am J Med Genet A, 2004. 126A(4): 413–9.
11. Thiele, H., et al., *Loss of chondroitin 6-O-sulfotransferase-1 function results in severe human chondrodysplasia with progressive spinal involvement.* Proc Natl Acad Sci U S A, 2004. 101(27): 10155–60.
12. Hermanns, P., et al., *Congenital joint dislocations caused by carbohydrate sulfotransferase 3 deficiency in recessive Larsen syndrome and humero-spinal dysostosis.* Am J Hum Genet, 2008. 82(6): 1368–74.
13. van Roij, M.H., et al., *Spondyloepiphyseal dysplasia, Omani type: further definition of the phenotype.* Am J Med Genet A, 2008. 146A(18): 2376–84.
14. Tuysuz, B., et al., *Omani-type spondyloepiphyseal dysplasia with cardiac involvement caused by a missense mutation in CHST3.* Clin Genet, 2009. 75(4): 375–83.
15. Unger, S., et al., *Phenotypic features of carbohydrate sulfotransferase 3 (CHST3) deficiency in 24 patients: congenital dislocations and vertebral changes as principal diagnostic features.* Am J Med Genet A, 2010. 152A(10): 2543–9.
16. Superti-Furga, A. and S. Unger, *Chondrodysplasia with Congenital Joint Dislocations, CHST3-Related*, in *GeneReviews((R))*, M.P. Adam, et al., Editors. 1993: Seattle (WA).
17. Otaify, G.A., et al., *CHST3-related skeletal dysplasia in 14 patients: Identification of 8 novel variants and further expansion of the phenotypic spectrum.* Am J Med Genet A, 2023. 191(8): 2100–2112.
18. Singh, S., et al., *Indian patients with CHST3-related chondrodysplasia with congenital joint dislocations.* Am J Med Genet A, 2024. 194(3): e63422.
19. Waryah, A.M., et al., *A novel CHST3 allele associated with spondyloepiphyseal dysplasia and hearing loss in Pakistani kindred.* Clin Genet, 2016. 90(1): 90–5.
20. Srivastava, P., et al., *Spondyloepiphyseal dysplasia Omani type: CHST3 mutation spectrum and phenotypes in three Indian families.* Am J Med Genet A, 2017. 173(1): 163–168.
21. Kausar, M., et al., *Biallelic variants in CHST3 cause Spondyloepiphyseal dysplasia with joint dislocations in three Pakistani kindreds.* BMC Musculoskelet Disord, 2022. 23(1): 818.
22. Mughal, T.A., et al., *A Novel Missense Variant in the CHST3 Underlies Spondyloepiphyseal Dysplasia with Congenital Joint Dislocations.* Mol Syndromol, 2024. 15(5): 355–361.
23. Pantoja-Melendez, C.A., et al., *Epidemiological and Molecular Characterization of a Mexican Population Isolate with High Prevalence of Limb-Girdle Muscular Dystrophy Type 2A Due to a Novel Calpain-3 Mutation.* PLoS One, 2017. 12(1): e0170280.
24. Duz, M.B. and A. Topak, *Recurrent c.776T>C mutation in CHST3 with four other novel mutations and a literature review.* Clin Dysmorphol, 2020. 29(4): 167–172.
25. Hackl, L., et al., *Homozygous DHCR7 p.Val330Met Variant Associated with Mild Non-Syndromic Intellectual Disability and Elevated Serum 7-Dehydrocholesterol Levels in Two Siblings.* Genes (Basel), 2025. 16(7).
26. Gudmundsson, S., et al., *Variant interpretation using population databases: Lessons from gnomAD.* Hum Mutat, 2022. 43(8): 1012–1030.
27. Ioannidis, N.M., et al., *REVEL: An Ensemble Method for Predicting the Pathogenicity of Rare Missense Variants.* Am J Hum Genet, 2016. 99(4): 877–885.
28. Rentzsch, P., et al., *CADD: predicting the deleteriousness of variants throughout the human genome.* Nucleic Acids Res, 2019. 47(D1): D886–D894.
29. Pejaver, V., et al., *Calibration of computational tools for missense variant pathogenicity classification and ClinGen recommendations for PP3/BP4 criteria.* Am J Hum Genet, 2022. 109(12): 2163–2177.
30. Jumper, J., et al., *Highly accurate protein structure prediction with AlphaFold.* Nature, 2021. 596(7873): 583–589.
31. Frappier, V., M. Chartier, and R.J. Najmanovich, *ENCoM server: exploring protein conformational space and the effect of mutations on protein function and stability.* Nucleic Acids Res, 2015. 43(W1): W395–400.
32. Gerasimavicius, L., X. Liu, and J.A. Marsh, *Identification of pathogenic missense mutations using protein stability predictors.* Sci Rep, 2020. 10(1): 15387.
33. Richards, S., et al., *Standards and guidelines for the interpretation of sequence variants: a joint consensus recommendation of the American College of Medical*

Genetics and Genomics and the Association for Molecular Pathology. Genet Med, 2015. 17(5): 405–24.
34. Tavtigian, S.V., et al., *Fitting a naturally scaled point system to the ACMG/AMP variant classification guidelines.* Hum Mutat, 2020. 41(10): 1734–1737.
35. Liang, H., et al., *A Chinese case of CHST3-related skeletal dysplasia and a systematic review.* Endocrine, 2023. 80(3): 658–668.
36. Bittles, A.H. and M.L. Black, *Evolution in health and medicine Sackler colloquium: Consanguinity, human evolution, and complex diseases.* Proc Natl Acad Sci U S A, 2010. 107 Suppl 1(Suppl 1): 1779–86.
37. Richard, I., et al., *Mutations in the proteolytic enzyme calpain 3 cause limb-girdle muscular dystrophy type 2A*. Cell, 1995. 81(1): 27–40.
38. Muys, J., et al., *Prenatal homozygosity mapping detects a novel mutation in CHST3 in a fetus with skeletal dysplasia and joint dislocations.* Clin Case Rep, 2017. 5(4): 440–445.
39. Tanteles, G.A., et al., *Two Somali half-siblings with CHST3-related chondrodysplasia illustrating the phenotypic spectrum and intrafamilial variability.* Am J Med Genet A, 2013. 161A(10): 2588–93.
40. Yan, W., et al., *Novel carbohydrate sulfotransferase 3 mutation causing spondyloepiphyseal dysplasia with congenital joint dislocations in a Chinese family.* . Ann Joint 2017. 2(2).
41. Ranza, E., et al., *Chondrodysplasia with multiple dislocations: comprehensive study of a series of 30 cases.* Clin Genet, 2017. 91(6): 868–880.
42. Van Biesen, N., P. Cools, and E. Meyers, *Comparison and Optimization of DNA Extraction Methods for Human DNA from Dried Blood Spot Samples.* Pediatr Rep, 2025. 17(2).
43. Jarvik, G.P. and B.L. Browning, *Consideration of Cosegregation in the Pathogenicity Classification of Genomic Variants.* Am J Hum Genet, 2016. 98(6): 1077–1081.